Optimizing LIGO with LISA forewarnings to improve black-hole spectroscopy

Rhondale Tso,* Davide Gerosa,† and Yanbei Chen‡
TAPIR 350-17, California Institute of Technology,
1200 E California Boulevard, Pasadena, CA 91125, USA
(Dated: July 3, 2018)

The early inspiral of massive stellar-mass black-hole binaries merging in LIGO's sensitivity band will be detectable at low frequencies by the upcoming space mission LISA. LISA will predict, with years of forewarning, the time and frequency with which binaries will be observed by LIGO. We will, therefore, find ourselves in the position of knowing that a binary is about to merge, with the unprecedented opportunity to optimize ground-based operations to increase their scientific payoff. We apply this idea to detections of multiple ringdown modes, or black-hole spectroscopy. Narrowband tunings can boost the detectors' sensitivity at frequencies corresponding to the first subdominant ringdown mode and largely improve our prospects to experimentally test the Kerr nature of astrophysical black holes. We define a new consistency parameter between the different modes, called δGR, and show that, in terms of this measure, optimized configurations have the potential to double the effectiveness of black-hole spectroscopy when compared to standard broadband setups.

Introduction– The first detections of merging black-hole (BH) binaries by the LIGO ground-based detectors [1] are one of the greatest achievement in modern science. Some of the inferred BH masses are as large as $\sim 30M_\odot$, and unexpectedly exceed those of all previously known stellar-mass BHs. These systems will also be visible by the future spaced-based detector LISA, which will soon observe the gravitational-wave (GW) sky in the mHz regime [2]. LISA will measure the early inspiral stages of BH binaries predicting, with years to weeks of forewarning, the time at which the binary will enter the LIGO band [3]. This will allow electromagnetic observers to concentrate on the source's sky location, thus increasing the likelihood of observing counterparts. Multi-band GW observations have the potential to shed light on BH-formation channels [4–8], constrain dipole emission [9], enhance parameter estimation [10] and provide new measurements of the cosmological parameters [11].

Here we explore the possibility of improving the science return of ground-based GW observations by combining LISA forewarnings to active interferometric techniques. LISA observations of stellar-mass BH binaries at low frequencies can be exploited to prepare detectors on the ground in their most favorable configurations for a targeted measurement. Optimizations can range from the most obvious ones (for instance just insuring the detectors are operational), to others that require more experimental work, like changing the input optical power, modifying mirror transmissivities and cavity tuning phases, and changing the squeeze factor and angle of the injected squeeze vacuum (see, e.g., [12]). Tuning the optical setup of the interferometer can allow to boost the signal-to-noise ratio (SNR) of specific features of the signal "on-demand" (only at the needed time, only at the needed frequency).

In particular, we apply this line of reasoning to the so-called *black-hole spectroscopy*: testing the nature of BHs through their ringdown modes. Narrowband tunings were previously explored to study the detectability of neutron-star mergers [13–15] and stochastic backgrounds [16], and are here applied to BH science for the first time.

The perturbed BH resulting from a merger vibrates at very specific frequencies. These quasi-normal modes of oscillation are damped by GW emission, resulting in the so-called BH ringdown [17, 18]. If BHs are described by the Kerr solution of General Relativity (GR) [19], all these resonant modes are allowed to depend on two quantities only: mass and spin of the perturbed BH [20–22]. This is a consequence of the famous *no-hair theorems*: as two BHs merge, all additional complexities (hair) of the spacetime are dissipated away in GWs, and a Kerr BH is left behind. The detection of frequency and decay time of one quasi-normal mode can therefore be used to infer mass and spin of the post-merger BH. Measurements of each additional mode provide consistency tests of the theory. This is the main idea behind BH spectroscopy: much like atoms' spectral lines can be used to identify nuclear elements and test quantum mechanics, quasi-normal modes can be used to probe the nature of BHs and test GR [23–26]. Despite its elegance, BH spectroscopy turns out to be challenging in practice as it requires loud GW sources and improved data analysis techniques [27–32].

The main idea behind our study is illustrated Fig. 1. A GW source like GW150914 emits GWs at ~ 0.1 Hz and is visible by LISA with SNR~ 5. After ~ 10 years, the emission frequency reaches ~ 10 Hz and the source appears in the LIGO band. The excitation amplitude of the dominant quasi-normal mode is ~ 10 times higher than the first subdominant mode. The latter is likely going to be too weak to perform BH spectroscopy. An optimized narrowband tuning can boost the detectability of the weaker mode at the expense of the rest of the signal, making BH spectroscopy possible.

* rtso@caltech.edu
† Einstein Fellow; dgerosa@caltech.edu
‡ yanbei@caltech.edu

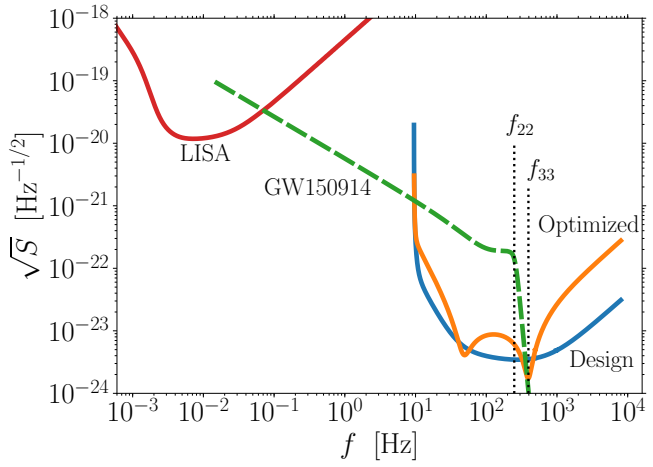

FIG. 1. GW amplitude $\sqrt{S_h} = 2|\tilde{h}|\sqrt{f}$ of a black-hole binary source similar to GW150914 compared to the noise curves $\sqrt{S_n}$ of LISA [33] and LIGO (both in its design, broadband configuration and with narrowband tunings). Optimized narrowbanding enhances (decreases) the detector sensitivity around the frequency f_{33} (f_{22}) of the first subdominant (dominant) mode of the BH ringdown. The BH binary waveform is generated using the approximant of [34] with $m_1 + m_2 = 65M_\odot$, $q = 0.8$, $D = 410$ Mpc, $\iota = 150°$ assuming optimal orientation ($\theta = \phi = \psi = 0$).

Black-hole ringdown– Let us consider a perturbed BH with detector-frame mass M and dimensionless spin j. GW emission during ringdown can be described by a superposition of damped sinusoids, labeled by $l \geq 2$, $0 \leq |m| \leq l$ and $n \geq 0$ [35]. For simplicity, we only consider the fundamental overtone $n = 0$.

Each mode is described by its frequency ω_{lm} and decay time τ_{lm}. The GW strain can be written as [36, 37]

$$h(t) = \sum_{l,m>0} B_{lm} e^{-t/\tau_{lm}} \cos\left(\omega_{lm} t + \gamma_{lm}\right) , \qquad (1)$$

$$B_{lm} = \frac{\alpha_{lm} M}{D} \sqrt{\left(F_+ Y_+^{lm}\right)^2 + \left(F_\times Y_\times^{lm}\right)^2} , \qquad (2)$$

$$\gamma_{lm} = \phi_{lm} + m\beta + \arctan\left(\frac{F_\times Y_\times^{lm}}{F_+ Y_+^{lm}}\right) , \qquad (3)$$

$$Y_{+,\times}^{lm}(\iota) = {}_{-2}Y_{lm}(\iota, \beta{=}0) \pm (-1)^l {}_{-2}Y_{l-m}(\iota, \beta{=}0) . \qquad (4)$$

where α_{lm} and ϕ_{lm} are the mode amplitudes and phases, D is the luminosity distance to the source, ${}_{-2}Y_{lm}(\iota, \beta)$ are the spin-weighted spherical harmonics, $F_{+,\times}(\theta, \phi, \psi)$ are the single-detector antenna patterns [38]. The angles ι and β describe the orientation of the BH, with ι (β) being the polar (azimuthal) angle measured with respect to the BH spin axis. In the conventions of [39, 40], the frequency-domain strain reads

$$\tilde{h}(f) = \sum_{l,m>0} B_{lm} \frac{-\omega_{lm} \sin\gamma_{lm} + (1/\tau_{lm} - i\omega)\cos\gamma_{lm}}{\omega_{lm}^2 - \omega^2 + 1/\tau_{lm}^2 - 2i\omega/\tau_{lm}} , \qquad (5)$$

where $f = \omega/2\pi$ is the GW frequency.

The dominant mode corresponds to l=2, m=2 (here after "22"), while the first subdominant is usually l=3, m=3 (hereafter "33"). Other modes might actually be stronger than the 33 mode for specific sources. For instance, the 33-mode is suppressed for $q \simeq 1$ or $\sin\iota \simeq 0$ (e.g [29, 41, 42]). Here we perform a simple two-mode analysis considering the 22 and 33 modes only. Our procedure can be straightforwardly generalized to sources where other modes dominate.

For simplicity, we restrict ourselves to non-spinning binary BHs with source-frame masses m_1 and m_2; we address the impact of this assumption below. Redshifted masses $m_i(1+z)$ are computed from the luminosity distance D using the Planck cosmology [43]. Mass M and spin j of the post-merger BH are estimated using fits to numerical relativity simulations [44, 45] as implemented by [46]. Quasi-normal frequencies ω_{lm} and decay times τ_{lm} are estimated from [25]. We estimate the excitation amplitudes α_{lm} given the mass ratio $q = m_2/m_1 \leq 1$ of the merging binary using the expressions reported by [37]. BH ringdown parameter estimation has been shown to depend very weakly on the phase offsets ϕ_{lm} [25], which we thus we set to 0 for simplicity (c.f. also [47]).

Narrowband tunings– As an example of a possible narrowband setup, we consider the detuning of the signal-recycling cavity (c.f. [14, 16] where a similar setup was also explored). Second-generation GW detectors make use of signal recycling optical configurations (or resonant side-band extraction) [48–50]. A signal recycling mirror is placed at the dark port of a Fabry-Perot Michelson interferometer, which is the configuration used in first-generation detectors. The transmittance $T_{\rm SRM}$ of this mirror determines the fraction of signal light which is sent back into the arms, possibly with a detuning phase $\phi_{\rm SRM}$. Both these parameters affect the optical resonance properties of the interferometer [48, 49], as well as its optomechanical dynamics [51, 52]. Together with the homodyne readout phase $\phi_{\rm hd}$, $T_{\rm SRM}$ and $\phi_{\rm SRM}$ are responsible for the quantum noise spectrum of the interferometer, allowing for noise suppression near optical and optomechanical resonances [53].

For concreteness, in this Letter we study narrowbanding of a single LIGO detector in its design configuration. More sensitive ground-based interferometers are currently being planned and are expected to be operational by the 2030s [54, 55]. Multi-band observations and LISA forewarnings are likely to happen with a network of ground-based detectors perhaps 5 or 10 times more sensitive than LIGO.

In order to select the best detuned configuration to perform BH spectroscopy, one needs to choose values of $(T_{\rm SRM}, \phi_{\rm SRM}, \phi_{\rm hd})$ that minimize the noise level around the 33 frequency, as illustrated in Fig. 1. We generate 60^3 noise curves with equal spacing in $\phi_{\rm SRM} \in [-0.12\pi, 0.12\pi]$, $T_{\rm SRM} \in [0.001, 0.2]$, and $\phi_{\rm hd} \in [0, \pi]$. This parameter space is capable of capturing the central frequencies of both the 22 and 33 mode for binaries with $q \in [0.2{-}0.9]$ and total masses $m_1{+}m_2 \in [20M_\odot{-}100M_\odot]$. Noise curves are generated using pyGWINC [56]. The LIGO design

configuration corresponds to $T_{\rm SRM}=0.2$, $\phi_{\rm SRM}=0$ and $\phi_{\rm hd}=\pi/2$. The broadband noise curves reported by [57, 58] are reproduced within $\Delta\log S_n/\log S_n \lesssim 0.2\%$ throughout the entire frequency band.

Mode Consistency– The main idea behind BH spectroscopy is to assume that quasi-normal modes frequencies ω_{lm} and decay times τ_{lm} depend separately on M and j, and then look for consistencies between the different estimates[1]. Considering the 22 and 33 modes only, one can write the waveform as $h=h_{22}(M_{22},j_{22})+h_{33}(M_{33},j_{33})$ and use data to estimate the parameters $\lambda=\{M_{22},j_{22},M_{33},j_{33}\}$. Here we present results of a Fisher analysis, which provide a conservative lower bound on the standard deviations [59] (but see [60]). The Fisher information matrix is defined as $\mathbf{\Gamma}_{ij}=(\partial\tilde{h}/\partial\lambda_i|\partial\tilde{h}/\partial\lambda_j)$, where parenthesis indicate the standard noise-weighted inner product. Standard deviations and correlations are given by $\sigma_i^2=\mathbf{\Gamma}^{-1}_{ii}$ and $\sigma_{ij}=\mathbf{\Gamma}^{-1}_{ij}$.

We propose two approaches to estimate consistency between the two modes.

(i) We first break the covariance matrix $\mathbf{\Gamma}^{-1}$ into blocks,

$$\mathbf{\Gamma}^{-1}=\begin{bmatrix}\mathbf{\Gamma}^{-1}_{2222} & \mathbf{\Gamma}^{-1}_{2233}\\ \mathbf{\Gamma}^{-1}_{3322} & \mathbf{\Gamma}^{-1}_{3333}\end{bmatrix} \tag{6}$$

corresponding to the couples $\{M_{22},j_{22}\}$ and $\{M_{33},j_{33}\}$. The diagonal blocks $\mathbf{\Gamma}^{-1}_{2222}$ and $\mathbf{\Gamma}^{-1}_{3333}$ can be used to construct confidences ellipses [61]. This procedure is useful to visually assess the accuracy of the two estimates, but fails to properly capture the correlations contained in the off-diagonal terms.

(ii) One can consider random variables $\delta\lambda_i$ describing fractional errors on the parameters of λ_i, such that their expectation values averaging over many realization is $\langle\delta\lambda_i\delta\lambda_j\rangle=\mathbf{\Gamma}^{-1}_{ij}/\lambda_i\lambda_j$. We construct the discrepancies on the mass and spin inferred from the two modes $\delta M=\delta M_{22}-\delta M_{33}$ and $\delta j=\delta j_{22}-\delta j_{33}$, and define the following estimator

$$\delta{\rm GR}=\left|\begin{matrix}\langle\delta M^2\rangle & \langle\delta M\delta j\rangle\\ \langle\delta j\delta M\rangle & \langle\delta j^2\rangle\end{matrix}\right|^{1/4} \tag{7}$$

to quantify the goodness of test of the theory. If the underlying theory of gravity is indeed GR (i.e. if $M_{22}=M_{33}\equiv M$ and $j_{22}=j_{33}\equiv j$), one obtains

$$\delta{\rm GR}=\frac{1}{\sqrt{Mj}}\Big[\left(\sigma^2_{M_{22}}-2\sigma_{M_{22}M_{33}}+\sigma^2_{M_{33}}\right)\left(\sigma^2_{j_{22}}-2\sigma_{j_{22}j_{33}}+\sigma^2_{j_{33}}\right)-\left(\sigma_{M_{22}j_{22}}+\sigma_{M_{33}j_{33}}-\sigma_{M_{22}j_{33}}-\sigma_{M_{33}j_{22}}\right)^2\Big]^{1/4}. \tag{8}$$

One has a perfect consistency test if $\delta{\rm GR}=0$, corresponding to $\mathbf{\Gamma}^{-1}=\mathbf{0}$. Large values of δGR imply poor constraints on the underlying theory. If correlations between the 22 and the 33 mode can be neglected (i.e. $\mathbf{\Gamma}^{-1}_{2233}\simeq\mathbf{\Gamma}^{-1}_{3322}\simeq 0$), δGR is proportional to (the square root of) the area of the confidence ellipse constructed from $\mathbf{\Gamma}^{-1}_{2222}+\mathbf{\Gamma}^{-1}_{3333}$. Given values of δGR from both a design and detuned configuration, we define the narrowband gain as

$$\zeta=\frac{\delta{\rm GR}^{\rm (Design)}-\delta{\rm GR}^{\rm (Optimized)}}{\delta{\rm GR}^{\rm (Design)}}\,, \tag{9}$$

where $\zeta=1$ ($\zeta=0$) means that the narrowbanding procedure is maximally effective (irrelevant).

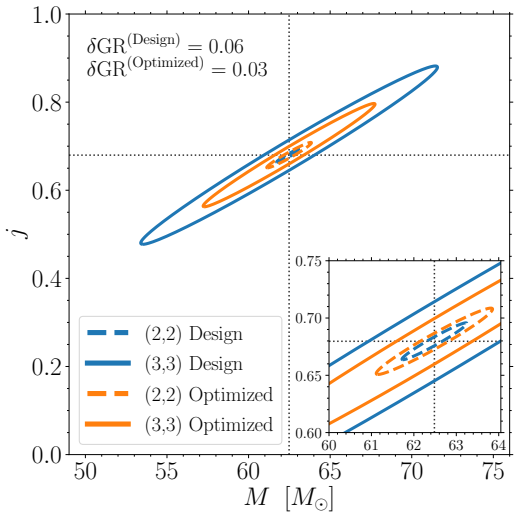

FIG. 2. 1-σ confidence ellipses for the 22 (dashed) and 33 (solid) modes observed by LIGO in its designed (blue) and optimized narrowband configuration (orange). The source is a perturbed Kerr BH of mass $M=62.5M_\odot$ and spin $j=0.68$ (dotted lines), resulting from the merger of a GW150914-like system ($m_1+m_2=65M_\odot$, $q=0.8$, $\iota=150^\circ$, $\beta=0$) assuming optimal orientation ($\theta=\phi=\psi=0$) and optimistic luminosity distance $D=40$ Mpc. The latter choice was made to mimic results from future-generation detectors.

Results– For each given source, we select the optimal noise curve that minimizes δGR among those we precomputed varying over tune phase, mirror transmittance, and homodyne phase. Figure 1 illustrates this procedure for an optimally oriented source similar to GW150914 [1]. This optimized narrowband setting corresponds to a noise curve with $\phi_{\rm SRM}\simeq 0.21$, $T_{\rm SRM}\simeq 0.02$ and $\phi_{\rm hd}\simeq 2.24$.

Confidence ellipses constructed from $\mathbf{\Gamma}^{-1}_{2222}$ and $\mathbf{\Gamma}^{-1}_{3333}$ are shown in Fig. 2 for a similar GW150914-like source but at the optimistic distance $D=40$ Mpc. This value is consistent with the closest GW source detected so far [62] and correspond to $\sim 1/10$ of the actual distance of GW150914. This choice makes the results of Fig. 2 indicative of detections with future ground-based detectors which are expected to take data in the 2030s together with LISA.

The behavior of the ellipses of Fig. 2 illustrates the

[1] For simplicity we only vary ω_{lm} and τ_{lm} while keeping α_{lm} fixed to their GR values.

main point of our analysis. In the standard broadband configuration, the 22 mode is observed very well, thus resulting in a small confidence region. At the same time, the 33 mode is observed poorly resulting in a large ellipse. As in the case of current events [63], this is roughly equivalent to a single measurement of M and j based on the 22 mode only, rather than a test of the theory. Narrowband tunings boost the detectability of the 33 mode, while marginally reducing that of the dominant 22 excitation. Consequently, the two confidence ellipses are more similar to each other, resulting in a more powerful constraint of the Kerr metric. For this specific source, narrowband tunings boost prospects to perform BH spectroscopy from $\delta\mathrm{GR} = 0.06$ to $\delta\mathrm{GR} = 0.03$, thus offering the opportunity to improve constraints on the BH no-hair theorems by $\zeta = 50\%$.

Let us now assess the impact of this procedure as a function of the source properties. We generate a population of sources drawing $\cos\theta$ and $\cos\iota$ uniformly in $[-1, 1]$ and β, ϕ and ψ uniformly in $[-\pi, \pi]$ with fixed[2] distance $D = 100$ Mpc. Fig. 3 shows the median values of δGR as a function of the masses of the merging BHs. The top panel assumes LIGO in its design configuration, the middle panel presents results optimizing the narrowband setup individually for each source, while the gain ζ is shown in the bottom panel.

A few interesting trends are present. First, the best systems to perform BH spectroscopy (i.e. low values of δGR) have intermediate mass ratio $0.3 \lesssim q \lesssim 0.7$. Both ringdown amplitudes α_{22} and α_{33} are suppressed for $q \to 0$, while $\alpha_{22} \gg \alpha_{33}$ for $q \to 1$. Second, tests of GR are weaker (higher δGR) for lower mass systems. These binaries have f_{33} close to the edge of the sensitivity window of the interferometer, thus making mode distinguishability harder. The LISA SNR also increases with the total mass: binaries with $m_1 + m_2 \lesssim 40 M_\odot$ are not likely to be associated with confirmed forewarnings.

A key point of our findings is illustrated in the gain values ζ reported in the bottom panel of Fig. 3. From Eq. (9), ζ quantifies the potential improvement in BH spectroscopy achievable with narrowband tunings. Median gains are larger than 25% over the entire parameter space, and individual sources can reach values up to 50%. In particular, higher gains are achieved for large-q systems. This agrees with the expectation that both modes are suppressed at $q \to 0$, while only the 33 mode is suppressed at $q \to 1$. Narrowband tunings shift the detector sensitivity closer to f_{33} at the expense of the 22 mode, and are thus more effective if its excitation is large such that the resulting sensitivity loss can be more easily absorbed.

Caveats– The possibility of optimizing ground-based operation assumes that LISA observations accurately predict

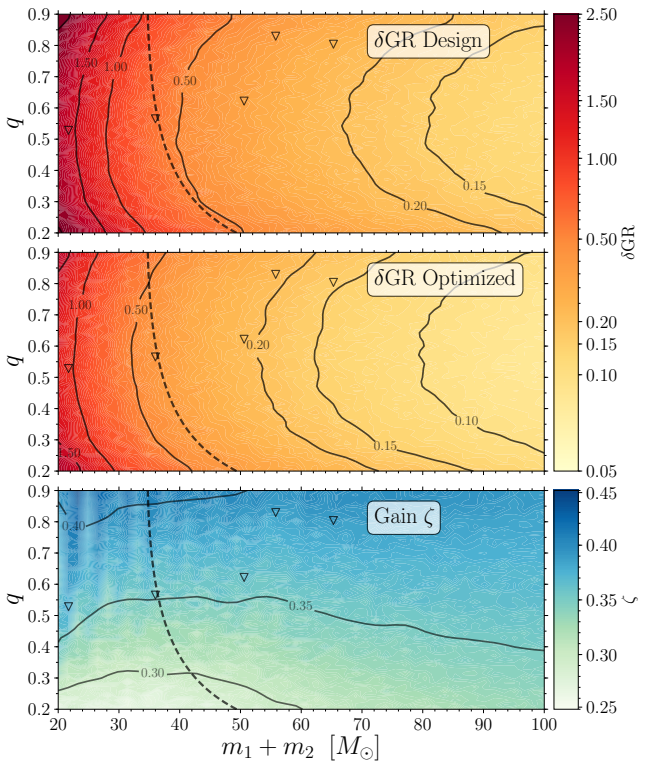

FIG. 3. Top and middle panels show median values of δGR for LIGO at design sensitivity and with narrowband tuning, respectively; bottom panel shows the median gain ζ. Data are shown as a function of total mass $m_1 + m_2$ and mass ratio q of the merging binaries; medians are computed over $\theta, \iota, \beta, \phi$ and ψ. The distance is fixed to $D = 100$ Mpc. Binaries to the right of the dashed lines have sky-averaged LISA SNRs greater than 8 (these are computed following [3] using the update noise curve of [33]; the initial frequency is estimated such that the binary merges in 5 years). Triangles indicate measured LIGO events [1, 64–67].

the ringdown frequencies (in particular f_{33}), thus providing information on *how* ground-based interferometers should be optimized. We estimate LISA errors on f_{33} as follows. For a given source with chirp mass M_c and symmetric mass ratio η, we first estimate f_{33} assuming zero spins (this is our working assumption used above). Inspired by the results reported in Fig. 3 of [3] (computed as in [68]), we model LISA errors as lognormal distributions centered at $\Delta M_c/M_c = 10^{-6}$, $\Delta\eta/\eta = 6\times10^{-3}$ with widths $\sigma = 0.5$. We then calculate f_{33} for a new binary with masses $M_c + \Delta M_c$ and $\eta + \Delta\eta$ and spins with magnitudes uniform in $[0, 1]$ and isotropic directions. In practice, we are assuming that LISA will not provide any information on the spins. This is a conservative, but realistic, assumption because spins enter at high post-Newtonian order and are probably going to be very challenging to detect at low frequencies. This procedure is iterated over a population of sources with masses uniformly distributed in $[10, 100] M_\odot$. The median of the errors Δf_{33} is 11 Hz, while the 90th percentile is 46 Hz. For the case of cavity

[2] Since δGR is directly proportional to D, results in Fig. 3 can be rescaled to different distances. Cosmological effects might push the ringdown frequencies of some high-mass events out of band, thus somewhat decreasing the gain.

detuning explored here, typical bandwidths are $\gtrsim 200$ Hz (c.f. Fig. 1), sensibly larger than the predicted errors. Therefore, we estimate that the risk of *missing* the source because the detector was detuned in the wrong configuration is very limited. The precision with which LISA will estimate the time of coalescence is at most of $\mathcal{O}(100\,\mathrm{s})$ [3], and should not pose significant challenges in the planning strategy.

Cavity detuning presents significant experimental challenges, regarding both detector characterization and lock acquisition, and might ultimately turn out to be impractical (see [69] for an exploration of these issues on the LIGO 40-m prototype). However, narrowband optimizations may not be limited to altering signal-recycling parameters, but can also involve other aspects of future ground-based inteferometers.

For the planned 3rd-generation detector Cosmic Explorer [55], the quantum noise is expected to dominate all other noise sources by more than a factor of 2 for frequencies $\gtrsim 40\,\mathrm{Hz}$ with a chosed bandwidth of 800 Hz. With forewarnings, a less broadband configuration (even without detuning) could be chosen to significantly improve BH spectroscopy. In the case of Einstein Telescope [54], a broad bandwidth is achieved by a xylophone that contains two different interferometers optimized for different frequency ranges. It is conceivable that a strong LISA forewarning might prompt a reconfiguration of the two interferometers to optimize for ringdown tests. Finally, we note that narrowbanding can also be achieved without detuning by using e.g. twin-recycling [70] or speed-meter [71] configurations; such a possibility is currently being studied to optimize for post-merger signals from neutron-star mergers for future detectors [15].

Conclusions– Space-based GW observatories like LISA will surely provide exquisite tests of GR with supermassive BH observations [25]. As shown here, they can further be exploited to improve BH spectroscopy in the different regime of lower-mass, higher-curvature BHs observed by LIGO and future ground-based facilities. More generally, forewarnings from space-based detectors will provide the opportunity to configure ground-based instruments to their most favorable configuration to perform targeted measurements and improve their science return.

Acknowledgements– We especially thank Jamie Rollins and Christopher Wipf for sharing their python port of the GWINC software. D.G. and Y.C. thank Christian Ott for important suggestions on the early developments of this idea. We also thank Rana Adhikari, Emanuele Berti, Jonathan Blackman, Neil Cornish, Matthew Evans, Matthew Giesler, Kevin Kuns, Lionel London, Belinda Pang, Alberto Sesana, Ulrich Sperhake, and Salvatore Vitale for fruitful discussions. R.T. is supported by the National Science Foundation Graduate Research Fellowship Program under Grant No. DGE-1144469, the Ford Foundation Predoctoral Fellowship, and the Gates Foundation. D.G. is supported by NASA through Einstein Postdoctoral Fellowship Grant No. PF6-170152 awarded by the Chandra X-ray Center, which is operated by the Smithsonian Astrophysical Observatory for NASA under Contract NAS8-03060.

[1] B. P. Abbott *et al.* (LIGO and Virgo Scientific Collaboration), PRL **116**, 061102 (2016), arXiv:1602.03837 [gr-qc].
[2] P. Amaro-Seoane *et al.* (LISA Core Team), (2017), arXiv:1702.00786 [astro-ph.IM].
[3] A. Sesana, PRL **116**, 231102 (2016), arXiv:1602.06951 [gr-qc].
[4] A. Nishizawa, E. Berti, A. Klein, and A. Sesana, PRD **94**, 064020 (2016), arXiv:1605.01341 [gr-qc].
[5] K. Breivik, C. L. Rodriguez, S. L. Larson, V. Kalogera, and F. A. Rasio, ApJ **830**, L18 (2016), arXiv:1606.09558.
[6] A. Nishizawa, A. Sesana, E. Berti, and A. Klein, MNRAS **465**, 4375 (2017), arXiv:1606.09295 [astro-ph.HE].
[7] X. Chen and P. Amaro-Seoane, ApJ **842**, L2 (2017), arXiv:1702.08479 [astro-ph.HE].
[8] K. Inayoshi, N. Tamanini, C. Caprini, and Z. Haiman, PRD **96**, 063014 (2017), arXiv:1702.06529 [astro-ph.HE].
[9] E. Barausse, N. Yunes, and K. Chamberlain, PRL **116**, 241104 (2016), arXiv:1603.04075 [gr-qc].
[10] S. Vitale, PRL **117**, 051102 (2016), arXiv:1605.01037 [gr-qc].
[11] W. Del Pozzo, A. Sesana, and A. Klein, MNRAS **475**, 3485 (2018), arXiv:1703.01300.
[12] R. X. Adhikari, Reviews of Modern Physics **86**, 121 (2014), arXiv:1305.5188 [gr-qc].
[13] S. A. Hughes, PRD **66**, 102001 (2002), gr-qc/0209012.
[14] H. Miao, H. Yang, and D. Martynov, (2017), arXiv:1712.07345 [gr-qc].
[15] D. Martynov, H. Miao, H. Yang, F. Hernandez, R. Adhikari, A. Freise, P. Lasky, Y. Levin, R. Smith, and E. Thrane, in preparation.
[16] D. Tao and N. Christensen, CQG **35**, 125002 (2018), arXiv:1801.02001 [gr-qc].
[17] C. V. Vishveshwara, Nature **227**, 936 (1970).
[18] E. Berti, V. Cardoso, and A. O. Starinets, CQG **26**, 163001 (2009), arXiv:0905.2975 [gr-qc].
[19] R. P. Kerr, PRL **11**, 237 (1963).
[20] W. Israel, Comm. Math. Phys. **8**, 245 (1968).
[21] B. Carter, PRL **26**, 331 (1971).
[22] M. Heusler, *Black hole uniqueness theorems, Cambridge University Press.* (1996).
[23] S. Detweiler, ApJ **239**, 292 (1980).
[24] O. Dreyer, B. Kelly, B. Krishnan, L. S. Finn, D. Garrison, and R. Lopez-Aleman, CQG **21**, 787 (2004), gr-qc/0309007.
[25] E. Berti, V. Cardoso, and C. M. Will, PRD **73**, 064030 (2006), gr-qc/0512160.
[26] E. Berti, K. Yagi, H. Yang, and N. Yunes, GRG **50**, 49 (2018), arXiv:1801.03587 [gr-qc].
[27] E. Berti, A. Sesana, E. Barausse, V. Cardoso, and K. Belczynski, PRL **117**, 101102 (2016), arXiv:1605.09286 [gr-

qc].
[28] A. Maselli, K. D. Kokkotas, and P. Laguna, PRD **95**, 104026 (2017), arXiv:1702.01110 [gr-qc].
[29] V. Baibhav, E. Berti, V. Cardoso, and G. Khanna, PRD **97**, 044048 (2018), arXiv:1710.02156 [gr-qc].
[30] H. Yang, K. Yagi, J. Blackman, L. Lehner, V. Paschalidis, F. Pretorius, and N. Yunes, PRL **118**, 161101 (2017), arXiv:1701.05808 [gr-qc].
[31] S. Bhagwat, M. Okounkova, S. W. Ballmer, D. A. Brown, M. Giesler, M. A. Scheel, and S. A. Teukolsky, (2017), arXiv:1711.00926 [gr-qc].
[32] R. Brito, A. Buonanno, and V. Raymond, (2018), arXiv:1805.00293 [gr-qc].
[33] N. Cornish and T. Robson, (2018), arXiv:1803.01944 [astro-ph.HE].
[34] S. Khan, S. Husa, M. Hannam, F. Ohme, M. Pürrer, X. J. Forteza, and A. Bohé, PRD **93**, 044007 (2016), arXiv:1508.07253 [gr-qc].
[35] S. A. Teukolsky, ApJ **185**, 635 (1973).
[36] E. Berti, J. Cardoso, V. Cardoso, and M. Cavaglià, PRD **76**, 104044 (2007), arXiv:0707.1202 [gr-qc].
[37] I. Kamaretsos, M. Hannam, S. Husa, and B. S. Sathyaprakash, PRD **85**, 024018 (2012), arXiv:1107.0854 [gr-qc].
[38] K. S. Thorne, in *Three Hundred Years of Gravitation*, 330-458 (1987).
[39] F. Echeverria, PRD **40**, 3194 (1989).
[40] L. S. Finn, PRD **46**, 5236 (1992), gr-qc/9209010.
[41] L. London, D. Shoemaker, and J. Healy, PRD **90**, 124032 (2014), [Erratum: PRD 94 6 069902 (2016)], arXiv:1404.3197 [gr-qc].
[42] S. Bhagwat, D. A. Brown, and S. W. Ballmer, PRD **94**, 084024 (2016), arXiv:1607.07845 [gr-qc].
[43] P. A. R. Ade *et al.* (Planck Collaboration), A&A **594**, A13 (2016), arXiv:1502.01589 [astro-ph.CO].
[44] E. Barausse, V. Morozova, and L. Rezzolla, ApJ **758**, 63 (2012), arXiv:1206.3803 [gr-qc].
[45] E. Barausse and L. Rezzolla, ApJ **704**, L40 (2009), arXiv:0904.2577 [gr-qc].
[46] D. Gerosa and M. Kesden, PRD **93**, 124066 (2016), arXiv:1605.01067 [astro-ph.HE].
[47] J. G. Baker, W. D. Boggs, J. Centrella, B. J. Kelly, S. T. McWilliams, and J. R. van Meter, PRD **78**, 044046 (2008), arXiv:0805.1428 [gr-qc].
[48] B. J. Meers, PRD **38**, 2317 (1988).
[49] G. Heinzel, J. Mizuno, R. Schilling, W. Winkler, A. Rüdiger, and K. Danzmann, Physics Letters A **217**, 305 (1996).
[50] G. Vajente, in *Advanced Interferometers and the Search for Gravitational Waves*, 404, 57 (2014).
[51] A. Buonanno and Y. Chen, PRD **65**, 042001 (2002), gr-qc/0107021.
[52] A. Buonanno and Y. Chen, PRD **67**, 062002 (2003), gr-qc/0208048.
[53] A. Buonanno and Y. Chen, PRD **64**, 042006 (2001), gr-qc/0102012.
[54] M. Punturo *et al.*, CQG **27**, 194002 (2010).
[55] B. P. Abbott *et al.* (LIGO and Virgo Scientific Collaboration), CQG **34**, 044001 (2017), arXiv:1607.08697 [astro-ph.IM].
[56] P. Fritschel, D. Coyne, *et al.*, dcc.ligo.org/T010075, git.ligo.org/gwinc/pygwinc.
[57] B. P. Abbott *et al.* (LIGO and Virgo Scientific Collaboration), LRR **19**, 1 (2016), arXiv:1304.0670 [gr-qc].
[58] D. Shoemaker *et al.*, dcc.ligo.org/LIGO-T0900288.
[59] C. Cutler and É. E. Flanagan, PRD **49**, 2658 (1994), gr-qc/9402014.
[60] C. L. Rodriguez, B. Farr, W. M. Farr, and I. Mandel, PRD **88**, 084013 (2013), arXiv:1308.1397 [astro-ph.IM].
[61] D. Coe, (2009), arXiv:0906.4123 [astro-ph.IM].
[62] B. P. Abbott *et al.* (LIGO and Virgo Scientific Collaboration), PRL **119**, 161101 (2017), arXiv:1710.05832 [gr-qc].
[63] B. P. Abbott *et al.* (LIGO and Virgo Scientific Collaboration), PRL **116**, 221101 (2016), arXiv:1602.03841 [gr-qc].
[64] B. P. Abbott *et al.* (LIGO and Virgo Scientific Collaboration), PRX **6**, 041015 (2016), arXiv:1606.04856 [gr-qc].
[65] B. P. Abbott *et al.* (LIGO and Virgo Scientific Collaboration), PRL **116**, 241103 (2016), arXiv:1606.04855 [gr-qc].
[66] B. P. Abbott *et al.* (LIGO and Virgo Scientific Collaboration), PRL **118**, 221101 (2017), arXiv:1706.01812 [gr-qc].
[67] B. P. Abbott *et al.* (LIGO and Virgo Scientific Collaboration), PRL **119**, 141101 (2017), arXiv:1709.09660 [gr-qc].
[68] E. Berti, A. Buonanno, and C. M. Will, PRD **71**, 084025 (2005), gr-qc/0411129.
[69] R. L. Ward, *Length sensing and control of a prototype advanced interferometric gravitational wave detector*, Ph.D. thesis, Caltech (2010).
[70] A. Thüring, C. Gräf, H. Vahlbruch, M. Mehmet, K. Danzmann, and R. Schnabel, Optics Letters **34**, 824 (2009), arXiv:1005.4650 [quant-ph].
[71] P. Purdue and Y. Chen, PRD **66**, 122004 (2002), gr-qc/0208049.